

# Molecular Dynamics Simulations of DNA Using the Generalized Born Solvation Model: Quantitative Comparisons with Explicit Solvation Results

Zara A. Sands and Charles A. Laughton\*

School of Pharmacy, University of Nottingham, University Park, Nottingham NG7 2RD, U.K.

Received: March 19, 2004

It is now well established that, with the correct treatment of hydration and long-range electrostatic effects, simulations of nucleic acid structure, dynamics, and recognition can yield remarkably reliable results and have genuine predictive power. While the “gold standard” remains modeling studies with the explicit treatment of water molecules and counterions, new implicit hydration models are being advanced as suitable choices for simulations where a shorter time-to-solution is required. In this study, we have evaluated the reliability of one such model, the generalized Born/surface area (GB/SA) continuum model by using it to study the interaction between the minor groove binding drug Hoechst 33258 and the DNA dodecamer d(CTTTTG-CAAAAG)<sub>2</sub>. There is extensive NMR and explicit hydrated modeling data on this system, and it shows the interesting property of highly cooperative binding of two molecules of the drug, such that the 1:1 complex is never observed. We find that with a suitable choice of parameters, the GB/SA model can perform adequately, reproducing the structural and dynamical characteristics observed in the previous explicitly solvated simulations in approximately a quarter of the computational time. However, limitations of this GB/SA method become apparent when the thermodynamic properties are evaluated.

## 1. Introduction

Solvent plays a crucial role in determining the structure and reactivity of biomacromolecules. The explicit inclusion of solvent molecules and the implementation of methods (e.g., particle-mesh Ewald) to treat long-range electrostatic interactions have been key issues for stable molecular dynamics (MD) simulations of nucleic acids on the nanosecond time scale and beyond.<sup>1–13</sup> For a typical explicitly solvated simulation, water may comprise 90% of the number of atoms to be included in the MD calculation, yet in many cases the atomistic dynamical behavior of individual solvent molecules is of no interest. For this reason there have been considerable efforts over recent years to develop simulation methods that permit the influence of the solvent on the structure and dynamics of the macromolecule to be included in an implicit way, at much reduced computational expense.<sup>14–17</sup>

In this study we have evaluated one such model, the generalized Born/surface area (GB/SA) model, developed by Still et al. and implemented in AMBER.<sup>18,19</sup> The total solvation free energy ( $\Delta G_{\text{sol}}$ ) can be expressed as the sum of a solute–solvent electrostatic term ( $\Delta G_{\text{pol}}$ ), a solvent cavity term ( $\Delta G_{\text{cav}}$ ), and a solute–solvent van der Waals term ( $\Delta G_{\text{vdw}}$ ):

$$\Delta G_{\text{sol}} = \Delta G_{\text{pol}} + \Delta G_{\text{cav}} + \Delta G_{\text{vdw}} \quad (1)$$

The generalized Born (GB) model provides an approximate solution to the first term in eq 1. The form implemented in AMBER6 is described by Tsui and Case<sup>16</sup> and includes a modification to allow for salt effects (at low concentrations) and a fast analytical method to estimate effective Born radii as a function of molecular conformation.<sup>20,21</sup> The last two terms in eq 1 account for the free energy associated with the formation of a cavity in the solvent and the changes in the dispersion

interactions that accompany solvation. These electrostatic terms are approximately proportional to the solvent-accessible surface area (SA) of the atom type,  $i$ , with a surface tension term,  $\sigma$ ,<sup>22</sup> set to 0.005 kcal/mol Å<sup>2</sup>.

$$\Delta G_{\text{cav}} + \Delta G_{\text{vdw}} = \sum \sigma_i(\text{SA})_i \quad (2)$$

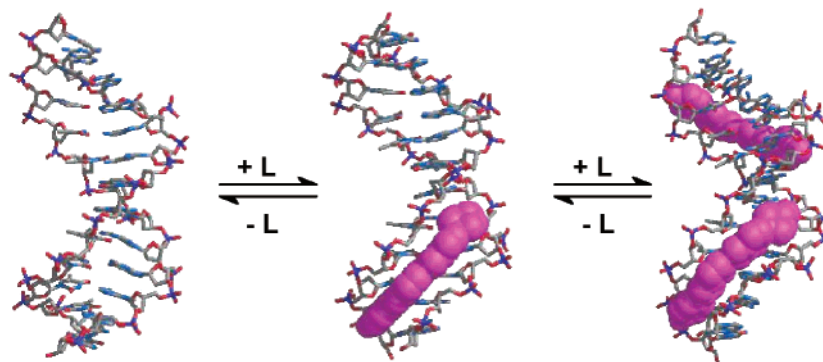
Here the SA term is calculated using the linear combination of pairwise orbitals approach (LCPO) algorithm. This is a fast analytical approximation for computing the exposed areas of atoms in molecules. Further details can be found in Still et al.<sup>23</sup>

Although this paper is concerned with the application of the GB approach to a nucleic acids system, it has been developed and applied to a wide variety of systems and problems. Thus, Gohlke et al. showed that postprocessing of MD data from explicitly solvated simulations using the GB/SA method provided fairly accurate values for the free energy of protein–protein interactions, if the ionic strength term was correctly chosen,<sup>24</sup> while Zhu et al. have described the parametrization of the GB/SA method to best reproduce the dynamics of a number of protein systems.<sup>25</sup> However, other studies have highlighted the potential limitations of the approach. For instance, Masumov and Lazaridis reported that the method, unsurprisingly, cannot reproduce the detail in the PMF profile between charged amino acid side chains (i.e., clear solvation shells),<sup>26</sup> while Jayaram et al. have shown that the parametrization of the method to give simultaneously both accurate solvation and interaction energies is not a trivial matter.<sup>27</sup>

In the area of nucleic acids simulations, a number of previous modeling studies have shown that the GB approach is capable of reproducing to good accuracy the structural characteristics of a number of nucleic acid systems also studied by explicitly solvated simulations.<sup>14,28,29</sup> However other GB studies of drug–DNA complexes have reported less satisfactory results.<sup>30</sup> Tsui and Case applied the GB model to MD simulations of a 10-

\* Corresponding author. E-mail: Charles.laughton@nottingham.ac.uk.

**SCHEME 1: Equilibria Involved in the Binding of Hoechst 33258 to d(CTTTTGCAAAAG)<sub>2</sub>, Where L Represents a Molecule of the Ligand**



base-pair duplex of DNA and RNA, resulting in stable trajectories whose structures, dynamics, and energetics were in close agreement with those seen in analogous explicitly solvated simulations.<sup>16</sup> Here we extend these investigations to an example of drug–DNA recognition, analyzing in more detail how the choice of parameters for GB/SA simulations affects their reliability and speed.

Recently we have used MD simulations to study the interaction between the minor groove binding ligand Hoechst 33258 and the DNA duplex d(CTTTTGCAAAAG)<sub>2</sub>.<sup>31</sup> NMR studies had shown that Hoechst binds to the two T<sub>4</sub>/A<sub>4</sub> tracts within this duplex in a highly cooperative manner, such that in titration experiments no intermediate 1:1 complex could be detected.<sup>32</sup> On the basis of this it could be concluded that the free energy change associated with the formation of the 2:1 complex from the 1:1 complex was at least 4.5 kcal/mol more negative than the formation of the 1:1 complex from the free DNA. The NMR-derived structures of the free DNA and the 2:1 complex were obtained but could shed little light on the origins of this cooperativity.<sup>33</sup> We performed a series of molecular dynamics simulations on the free DNA, the 1:1 complex, and the 2:1 complex (Scheme 1) using an explicit hydration model. The experiments were designed such that the key thermodynamic parameters associated with the cooperativity ( $\Delta\Delta G$  and its enthalpic and entropic components) could be calculated. The results of this MD study confirmed that structural factors alone could not explain the cooperativity observed; indeed when enthalpic and hydration factors were looked at in isolation, the recognition process was predicted to be slightly anticooperative. However, when changes in configurational entropy were taken into account, the overall free energy differences were such that the calculated cooperativity was in good agreement with that observed experimentally.

In this study the ensembles for the thermodynamic analyses were generated from extended MD simulations using an explicit solvation model. However, for the energetic analyses themselves the configurations were reanalyzed using the GB/SA method so that solvation free energy terms could be evaluated. It occurred to us that an attempt to repeat the same study, using the GB/SA approach throughout, would represent a more challenging and further-reaching test as to the utility and reliability of the GB/SA method than any previously reported investigation.

The results of this work are presented here. The influence of key parameters associated with the GB/SA method have been investigated and a set of benchmarks established against which the performance capabilities of different simulation protocols can be measured. The benchmarks permit two simulations to be compared quantitatively for similarity in static, dynamic, and

thermodynamic behavior. The results obtained throw light onto the reliability of the GB/SA approach as a substitute for relatively expensive explicitly solvated simulations of DNA, indicating how they can be optimized and where their strengths and limitations lie.

## 2. Methods

**2.1. Molecular Dynamics Simulations.** All simulations were performed using the AMBER6 suite of programs,<sup>19</sup> running on Silicon Graphic workstations. Equilibrated systems generated by Harris<sup>31</sup> were used to initiate MD simulations. Calculations were carried out using the Sander module with SHAKE applied to constrain all bonds, allowing a 2 fs time step. Simulations were performed using the Berendsen temperature-coupling algorithm to maintain a constant temperature of 300 K.<sup>34</sup> In each case a 10 ps equilibration run was carried out to enable the system to warm to 300 K, after which the production simulation was performed. The VMD program was used for molecular visualization.<sup>35</sup>

**2.2. Benchmarking Measures.** To guide the GB/SA parameter optimization process, we implemented a series of measures that would enable us to quantitatively assess the similarity between the structural, dynamical, and thermodynamic properties calculated from simulations of the implicitly solvated systems and those of their explicitly solvated counterparts, taken from our previous work.<sup>31</sup>

**2.2.1. Structural Comparisons.** To examine general structural similarity, all atom time-averaged structures of the DNA component were calculated from each GB/SA simulation and the root-mean-square deviation (rmsd) of the atomic coordinates were calculated from the corresponding structures obtained via the explicitly solvated MD simulations.

**2.2.2. Dynamical Comparisons.** To examine detailed dynamical similarity, principal component analysis (PCA) was performed on the acquired DNA structures, using the method described previously.<sup>31</sup> A similar analysis method has been applied to the study of an RNA duplex by Sherer and Cramer and to a protein system by Cornell et al.<sup>36,37</sup> Briefly, from the equilibrated portion of each trajectory, a  $3N \times 3N$  covariance matrix of the Cartesian coordinates was generated and then diagonalized to give  $3N$  eigenvectors. The eigenvectors provide a vectorial representation of each mode of structural deformation, and the corresponding eigenvalue indicates the relative contribution made by that mode to the motion as a whole. Typically, the first 10 eigenvectors capture 80–90% of the total variance, and so an analysis of dynamics can concentrate on these.

Overlaps between the subspaces spanned by the top 10 eigenvectors of corresponding explicitly and implicitly solvated

simulations were quantified using the method described by Hess.<sup>38</sup> For two sets of  $n$  orthogonal vectors  $\mathbf{v}_1, \dots, \mathbf{v}_n$  and  $\mathbf{w}_1, \dots, \mathbf{w}_n$ , the overlap is given by

$$\text{overlap}(\mathbf{v}, \mathbf{w}) = \frac{1}{n} \sum_{i=1}^n \sum_{j=1}^n (v_i \cdot w_j)^2 \quad (3)$$

When sets  $\mathbf{v}$  and  $\mathbf{w}$  span the same subspace, the overlap is 1.

**2.2.3. Thermodynamic Comparisons.** The nature of the equilibria we were investigating was such that we could calculate the difference between the free energy changes associated with the first and second binding events ( $\Delta\Delta G$ ) without having to characterize the thermodynamics of the unbound drug. The total free energy term can be expanded as shown in eq 4:

$$G = E_{\text{intra}} + G_{\text{solv}} - TS_{\text{intra}\infty} \quad (4)$$

The first term,  $E_{\text{intra}}$ , is the internal energy of the solute (DNA or DNA–drug complex), the second term,  $G_{\text{solv}}$ , is the free energy of solvation of the solute, and the third term,  $S_{\text{intra}\infty}$ , is the configurational entropy at  $t_{\infty}$  of the solute (see below). With the use of eq 4 and the scheme depicted in Scheme 1, the free energy difference that measures the cooperativity can be computed as shown in eq 5:

$$\Delta\Delta G = (E_{\text{intra}} + G_{\text{solv}})_0 + (E_{\text{intra}} + G_{\text{solv}})_2 - 2(E_{\text{intra}} + G_{\text{solv}})_1 - T(S_{\text{intra}\infty 0} + S_{\text{intra}\infty 2} - 2S_{\text{intra}\infty 1}) \quad (5)$$

where 0 represents the free DNA system, 1 represents the 1:1 Hoechst–DNA complex, and 2 represents the 2:1 Hoechst–DNA complex.

The  $(E_{\text{intra}} + G_{\text{solv}})$  terms were obtained directly from the GB/SA simulation output, while the eigenvalues from the PCA were used to compute configurational entropies according to the method of Schlitter:<sup>39</sup>

$$S_{\text{intra}} = 0.5k \ln(\pi[1 + (kT\epsilon^2/\hbar^2)s_{ij}]) \quad (6)$$

where  $S_{\text{intra}}$  is the configuration entropy,  $k$  is Boltzmann's constant,  $T$  is temperature,  $\hbar$  is Planck's constant/ $2\pi$ , and  $s_{ij}$  are the mass-weighted classical variances.

Entropy values obtained in this way are inherently sensitive to simulation length. To correct for this, entropies were calculated for different window widths (500 ps to 4 ns) and extrapolated to  $t_{\infty}$ , using the empirical relationship

$$S_{\text{intra}}(t) = S_{\text{intra}\infty} - \frac{\alpha}{t^{2/3}} \quad (7)$$

where  $\alpha$  is a fitting parameter.

### 3. Results and Discussion

**3.1. Selection of Parameters.** The GB model as implemented in AMBER 6.0 offers the option to include or exclude the nonpolar (SA) contributions to the  $\Delta G_{\text{solv}}$  term. Including it requires a relatively expensive calculation of solvent-accessible surface areas at each time step, and it has been suggested that where free energy differences are required rather than absolute values, it may be omitted as resulting errors may be expected to cancel out. There are other adjustable variables in this application of the GB model—in particular ionic concentration and the cutoff distance for calculating effective Born radii (and nonbonded interactions). Before a full thermodynamic study was performed we sought to identify those parameters that when applied in this continuum approach would enable MD simulation

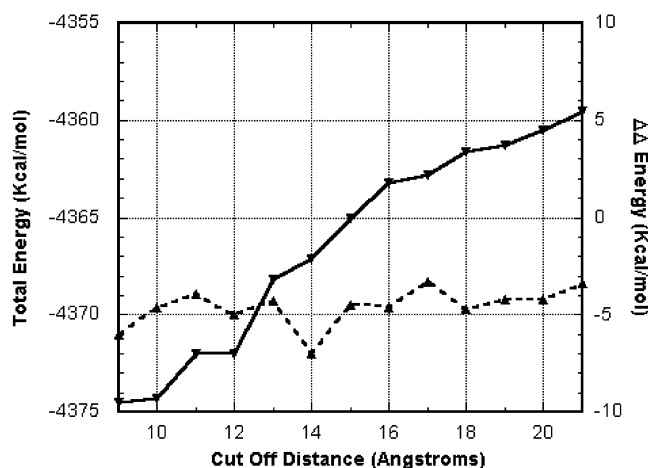


**Figure 1.** Effect of nonbonded cutoff distance on the calculated total internal energy of the free DNA system (solid line) and the difference in internal energy between the two binding events (dashed line): see eq 5 and Figure 1.

of the DNA/Hoechst system to be performed as fast as possible, while producing structural and dynamical properties comparable to those acquired using the explicitly solvated approach.

**3.1.1. Ionic Concentration.** Salt contributions are known to influence the structural and dynamic characteristics of duplex DNA.<sup>40,41</sup> Successful GB studies have been conducted employing 0.2 M salt concentration.<sup>14,16,28</sup> In vitro DNA–ligand binding studies are often conducted using ionic concentrations in the range of 0.00–0.20 M.<sup>42</sup> With these values in mind we decided to consider the effects of implementing 0.2 and 0.02 M salt concentrations.

**3.1.2. Cutoff Distance.** A variable commonly adjusted to control the speed versus accuracy of both vacuum and explicit solvent simulations is the cutoff value in distances between atomic pairs for evaluating nonbonded interactions. In AMBER, the cutoff parameter for GB simulations controls not only the truncation of Coulombic and Lennard-Jones parameters but also the exclusion of distant pairs of atoms in computing the effective Born radii.

Single-point energy calculations were performed on the representative conformations of the free d(CTTTTGCAAAG)<sub>2</sub> duplex and the 1:1 and the 2:1 Hoechst–DNA complexes. For each energy calculation, the cutoff distance for each system was systematically increased by 1 Å, from 9 to 21 Å inclusive, while implementing the surface area term and an ionic concentration of 0.2 M.

As expected (Figure 1), the total energies ( $E_{\text{total}} = E_{\text{intra}} + G_{\text{solv}}$ ) of the systems were sensitive to the nonbonded cutoff distance. However, the  $\Delta\Delta E_{\text{total}}$  between the three discrete systems was found to be essentially independent of the cutoff value, which is the important consideration for the purpose of this study. Cutoff distance values of 9, 12, and 15 Å were then arbitrarily chosen for further evaluation.

**3.2. Investigation of Parameters.** Combinations of cutoff distances, ionic concentrations, and use or otherwise of the surface area term were then applied to 2 ns MD simulations of the free DNA and the 2:1 drug–DNA complex (see Table 1). Animations of the trajectories acquired for the free DNA simulations (I–VIII, Table 2) revealed that the integrity of the DNA duplex was maintained for all but three runs (I, V, and VII). Analogous analyses of the 2:1 drug DNA/complex simulations (IX–XVI) illustrated that the duplex structure of the DNA was maintained in every case. It is interesting to observe that simulation protocols unsuitable for the free DNA



**TABLE 1: Simulation Protocols Used to Investigate the Influence of Key GB/SA Parameters**

| protocol | SA term | cutoff ( $\text{\AA}$ ) | ionic strength (M) |
|----------|---------|-------------------------|--------------------|
| A        | on      | 9                       | 0.2                |
| B        | off     | 9                       | 0.2                |
| C        | on      | 12                      | 0.2                |
| D        | on      | 9                       | 0.02               |
| E        | off     | 12                      | 0.2                |
| F        | off     | 15                      | 0.2                |
| G        | off     | 9                       | 0.02               |
| H        | on      | 15                      | 0.2                |

**TABLE 2: Analysis of the 2 ns MD Simulations Performed on the (Implicitly Solvated) Free DNA System and the 2:1 Drug–DNA Complex<sup>a</sup>**

| simulation | drug–DNA ratio | protocol | stable <sup>b</sup> | rmsd ( $\text{\AA}$ ) | PCA overlap | speed-up <sup>c</sup> |
|------------|----------------|----------|---------------------|-----------------------|-------------|-----------------------|
| I          | 0              | A        | no                  | 1.38                  | 0.62        | 1.96                  |
| II         | 0              | B        | yes                 | 0.80                  | 0.73        | 3.53                  |
| III        | 0              | C        | yes                 | 0.65                  | 0.65        | 1.66                  |
| IV         | 0              | D        | yes                 | 0.65                  | 0.64        | 2.09                  |
| V          | 0              | E        | no                  | 1.01                  | 0.62        | 2.44                  |
| VI         | 0              | F        | yes                 | 0.88                  | 0.78        | 1.88                  |
| VII        | 0              | G        | no                  | 1.56                  | 0.50        | 3.56                  |
| VIII       | 0              | H        | yes                 | 0.72                  | 0.75        | 1.37                  |
| IX         | 2              | A        | yes                 | 1.01                  | 0.76        | 1.86                  |
| X          | 2              | B        | yes                 | 0.81                  | 0.75        | 3.31                  |
| XI         | 2              | C        | yes                 | 0.99                  | 0.77        | 1.45                  |
| XII        | 2              | D        | yes                 | 0.95                  | 0.76        | 1.86                  |
| XIII       | 2              | E        | yes                 | 0.77                  | 0.78        | 2.26                  |
| XIV        | 2              | F        | yes                 | 0.67                  | 0.78        | 1.73                  |
| XV         | 2              | G        | yes                 | 0.68                  | 0.76        | 3.32                  |
| XVI        | 2              | H        | yes                 | 0.86                  | 0.80        | 1.22                  |

<sup>a</sup> Values for RMSD, PCA, overlap, and speed-up are all relative to the corresponding simulation performed using explicit solvent. <sup>b</sup> If during the course of a trajectory DNA base pair(s) separated and remained so for the remainder of the trajectory, the system was deemed to be unstable. <sup>c</sup> Relative increase in the speed of the computation of an MD simulation relative to the analogous explicitly solvated calculation.<sup>26</sup>

were satisfactory for the simulation of the 2:1 complex. One plausible reason could be that GB/SA simulations seem prone to instability when extreme conformations of the duplex are sampled. Other studies have also shown that increased structural fluctuations are commonly observed in GB simulations compared to explicitly solvated ones.<sup>14,25,37</sup> When two molecules of Hoechst bind in the minor groove of the DNA, they reduce the flexibility of the duplex and so the sampling of such regions. This is discussed further below.

The rmsd values in Table 2 give a general picture of how well the GB/SA simulations could reproduce the time-averaged structural properties found from the previous explicitly solvated simulations. To put these values into context, we found that if the previously acquired 4 ns explicitly solvated trajectories of the free DNA and 2:1 complex were divided into two halves and the resultant time-averaged DNA structures compared, we obtained rmsd values of 0.46 and 0.61  $\text{\AA}$  for each system, respectively. With these threshold values in mind we see that many of the stable implicitly solvated simulations produce time-averaged structures that are only just distinguishable from their explicitly solvated counterparts.

PCA was performed on the DNA duplexes taken from each simulation (excluding the drug molecules, where present). As expected, the majority of the total variance, over 80% for each system, was captured by considering just the top 10 eigenvectors (results not detailed in this communication). Therefore, as a measure of overall dynamical similarity to the explicitly solvated simulations, these eigenvectors were used to calculate the PC

overlap. Again, for comparison, when the 4 ns trajectories from the explicitly solvated free and 2:1 drug/DNA simulations were split in two and PCA performed independently on each, the eigenvector overlap values between the corresponding halves were found to be 0.72 and 0.82, respectively. Table 2 shows that, with respect to the free DNA systems, simulations II, VI, and VIII had scores over 0.72, indicating dynamics essentially indistinguishable from that obtained using explicit solvent. For the 2:1 drug/DNA systems, although the overlap values were below 0.82, the majority of the results were very close to this threshold value.

The calculation of PC overlaps indicates that the modes of deformation of the DNA found in GB/SA simulations match very well to those observed using explicit solvent. However, Figure 2 shows how the projections of the top three eigenvectors vary during the course of an MD run for simulation II and the corresponding explicitly solvated simulation. The implicitly solvated example chosen here typifies the deformation characteristics observed for all simulations employing the GB/SA methodology. It is evident that although both simulation strategies lend to very similar modes of deformation they explore these modes in radically different ways. The dynamics in the GB/SA simulations are characterized by regular harmonic motions with a well-defined frequency, while for the explicitly solvated systems the motion is highly erratic, being dominated by frictional and stochastic effects from the surrounding explicitly modeled solvent environment.

All GB/SA simulations were faster than the explicitly solvated benchmark, but the speed-up varied from a relatively modest 1.2-fold to a more impressive factor of 3.6. As expected, it was found that the use of the surface area term was computationally expensive, increasing the simulation time by a factor of 1.4–1.8. When the surface area term was used, the simulation time was relatively insensitive to the nonbonded cutoff, increasing by a factor of about 1.2 on going from 9 to 12  $\text{\AA}$ , and by a factor of about 1.4 on going from 9 to 15  $\text{\AA}$ . In contrast, if this term was not used the corresponding factors were 1.5 and 1.9, respectively. Changes in ionic strength had a negligible effect upon computation times.

The ultimate aim of this testing phase, as mentioned above, was to determine which parameters, when employed in this continuum solvation approach, would enable an MD simulation to be performed as rapidly as possible, while producing results comparable with those acquired using the explicitly solvated method. With this in mind we considered that protocols B, F, and H outperformed all others.

**3.3. Thermodynamic Calculations.** The three experimentally determined optimal protocols, namely, B, F, and H, were further applied to 4 ns MD simulations of the free DNA system, the 1:1 complex, and the 2:1 complex, to see if they could reproduce the thermodynamic quantities associated with the Hoechst 33258–DNA binding process that were calculated in our previous explicitly solvated simulations.

The trajectories acquired from the simulations implementing protocols B, F, and H revealed that the duplex structure of the DNA remained intact during the course of each run. However, there was one exception. Inspection of the trajectory acquired for the 1:1 complex, using protocol H, revealed that the DNA had frayed irreversibly. Having a poorly represented 1:1 complex, we decided that protocol H should not be considered any further in this investigation.

**3.3.1. Internal Energy and Solvation Terms.** The internal energies with solvation correction ( $E_{\text{intra}} + G_{\text{solv}}$ ) were calculated for the free DNA and the 1:1 and the 2:1 complexes by

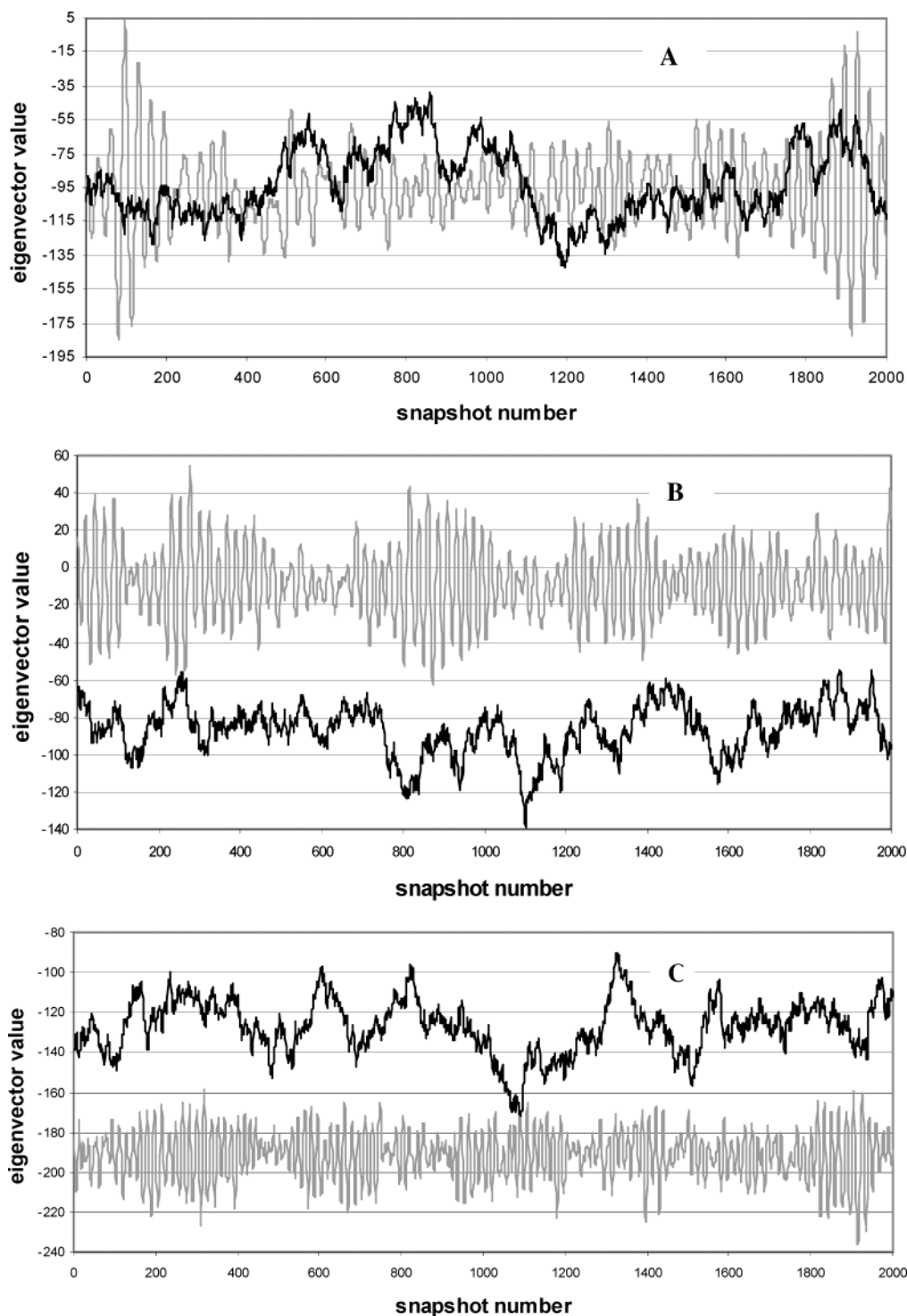


**Figure 2.** Graphs A, B, and C depict how principal components 1, 2, and 3, respectively, acquired from simulation II (black) and the corresponding explicitly solvated simulation (gray) vary during the course an MD run.

analyzing each snapshot of the generated trajectories. The  $\Delta\Delta(E_{\text{intra}} + G_{\text{solv}})$  values were then determined for each systems using protocols B and F. As shown in Table 3, protocols B and F yielded slightly negative  $\Delta\Delta(E_{\text{intra}} + G_{\text{solv}})$  values. Thus on the basis of enthalpy considerations (including a solvation correction), the implicitly solvated simulations predict the interaction of Hoechst 33258 with this DNA sequence to be weakly cooperative, in disagreement with the prediction from the explicitly solvated simulations. However, we found that when each snapshot of the simulations produced under protocol F was postprocessed to recalculate the internal energy with the

inclusion of the surface area term, the resultant  $\Delta\Delta(E_{\text{intra}} + G_{\text{solv}})$  term was predictive of a weakly anticooperative binding event.

**3.3.2. Calculation of Configurational Entropies.** Configurational entropy changes ( $\Delta S_{\text{intra}\infty}$ ) of the free DNA, the 1:1 complex, and the 2:1 complex were determined using the approach detailed in section 2.2.3.

From these results we calculated  $T\Delta\Delta S_{\text{intra}\infty}$  at 300 K to be  $-24.1$  and  $12.7$  kcal/mol/K for the simulation produced using protocols B and F, respectively. As shown in Table 3, the entropy value deduced using condition B was neither in qualitative or quantitative agreement with the explicitly solvated

**TABLE 3: Thermodynamic Parameters (All in kcal/mol) of the Hoechst 33258–DNA Binding Process, Calculated under Varying Conditions**

| protocol         | $\Delta\Delta(E_{\text{intra}} + G_{\text{solv}})$ | $T\Delta\Delta S_{\text{intra}\infty}$ | $\Delta\Delta G$ |
|------------------|--|--|------------------|
| explicit solvent | 3.2  | 10.4                                   | −7.2             |
| B                | −0.1   | −24.1                                  | 24.0             |
| F                | −0.6   | 12.7                                   | −13.3            |
| F* <sup>a</sup>  | 1.4  | 12.7                                   | −11.3            |

<sup>a</sup> Postprocessing of trajectories acquired implementing protocol F, with the inclusion of the SA term.

value. Although protocol F was not in quantitative agreement, it was in qualitative agreement with the explicitly hydrated result, predicting a cooperative recognition process based on the  $T\Delta\Delta S_{\text{intra}\infty}$  term alone.

**3.3.3. Free Energy Differences.** The free energy changes upon binding were calculated using eq 5. From NMR titration studies we know that  $\Delta\Delta G$  for the binding process must be −4.5 kcal/mol or more negative. Clearly, GB/SA simulation protocol B led to a seriously erroneous result. Against the benchmark of the explicitly solvated simulations, protocol F (15 Å cutoff, no surface area term, 0.2 M ionic strength) performed much better but was still only qualitatively correct. Reprocessing the simulation data to add the surface area correction (F\*) improved the agreement somewhat. However, one could argue that, at least for this analysis, the benchmark should be the NMR-derived result, in which case we cannot say whether protocol F or F\* gives results that are better or worse than those from the explicitly solvated simulation, only that they are different.

#### 4. Conclusions

This investigation has made it clear that the utility and reliability of the GB/SA method as a computationally efficient alternative to explicitly solvated simulations is critically dependent on exactly what information it is desired to extract from the study. Satisfactory structural characteristics can be obtained quite consistently, while satisfactory dynamical characteristics require more care. It may be argued that, at least for this extremely testing investigation, satisfactory thermodynamic characteristics were not obtained for any of the combinations of GB/SA parameters investigated, though it was possible to reproduce the important qualitative conclusion from the explicitly solvated simulations study—that the cooperativity of ligand binding was entropy, not enthalpy, driven.

The computational advantage of using the GB/SA method for such studies is rather variable. Where only structural data is required, parameters giving a more than 3-fold increase in speed may suffice. But if dynamical or even thermodynamical analysis is the aim, satisfactory parameters for the simulations may result in a less than 2-fold speed-up. Somewhat surprisingly, there is not an obvious relationship between the choice of simulation parameters and the quality of the results. Perhaps the clearest example of this comes from the failure of the most “expensive” protocol, implementing the surface area term and a 15 Å cutoff (H), to produce a simulation of the 1:1 drug–DNA complex that is stable over 4 ns. In general GB/SA simulations appear more “fragile” than explicitly solvated ones. All the simulations reported here began from configurations that had been well equilibrated through previous explicitly solvated simulations. Other simulations, not reported here, which began from unequilibrated structures, proved very prone to dynamical instability. It seems very likely that this is due to the absence of solvent-induced damping of molecular motions in such simulations, as illustrated in Figure 2. This clearly illustrates

the area in which such implicitly solvated simulations diverge most radically from their explicitly solvated counterparts—their time-dependent behavior. Indeed, it has been argued that the concept of a time step in implicitly solvated simulations has little meaning, as the solvent is being treated in a time-averaged way.<sup>16</sup> It seems reasonable to suppose that the introduction of a solvent damping term would result in more “realistic” dynamical behavior, could lead to more robust simulations, and might improve thermodynamic analyses of the data. However, to introduce such a term can be expected to erode yet further the relatively modest improvement in computational efficiency that the use of such models gives.

**Acknowledgment.** This work was supported by the UK Biotechnology and Biological Sciences Research Council (BBSRC) and the Environmental and Physical Sciences Research Council (EPSRC).

#### References and Notes

- (1) Cheatham, T. E., III; Miller, J. L.; Fox, T.; Darden, T. A.; Kollman, P. A. *J. Am. Chem. Soc.* **1995**, *117*, 4193–4194.
- (2) Cheatham, T. E., III; Kollman, P. A. *J. Am. Chem. Soc.* **1997**, *119*, 4805–4825.
- (3) Young, M. A.; Ravishanker, G.; Beveridge, D. L. *Biophys. J.* **1997**, *73*, 2313–2336.
- (4) Beveridge, D. L.; McConnell, K. L. *Curr. Opin. Struct. Biol.* **2000**, *10*, 182–196.
- (5) Cheatham, T. E., III; Kollman, P. A. *Annu. Rev. Phys. Chem.* **2000**, *51*, 435–471.
- (6) York, D. M.; Yang, W.; Lee, H.; Darden, T. A.; Pedersen, L. G. *J. Am. Chem. Soc.* **1995**, *117*, 5001–5002.
- (7) Cheatham, T. E., III; Miller, J. L.; Spector, T. I.; Cieplak, P.; Kollman, P. A. In *Molecular Modeling of Nucleic Acids*; Leontis, N. B., SantaLucia, J., Eds.; American Chemical Society: Washington, DC, 1998; pp 285–303.
- (8) Beveridge, D. L.; Young, M. A.; Sproun, D. In *Molecular Modeling of Nucleic Acids*; Leontis, N. B., SantaLucia, J., Eds.; American Chemical Society: Washington, DC, 1998; pp 260–284.
- (9) Mackerell, A. D., Jr. In *Molecular Modeling of Nucleic Acids*; Leontis, N. B., SantaLucia, J., Eds.; American Chemical Society: Washington, DC, 1998; pp 2304–311.
- (10) Yang, L.; Pettitt, B. M. *J. Phys. Chem.* **1996**, *100*, 2564–2566.
- (11) Feig, M.; Pettitt, B. M. *J. Phys. Chem. B* **1997**, *101*, 7361–7363.
- (12) Feig, M.; Pettitt, B. M. *Biophys. J.* **1998**, *75*, 134–149.
- (13) Feig, M.; Pettitt, B. M. *Biophys. J.* **1999**, *77*, 1769–1781.
- (14) Tsui, V.; Case, D. A. *Biopolymers* **2001**, *56*, 275–291.
- (15) Bashford, D.; Case, D. A. *Annu. Rev. Phys. Chem.* **2000**, *51*, 129–152.
- (16) Tsui, V.; Case, D. A. *J. Am. Chem. Soc.* **2000**, *122*, 2489–2498.
- (17) Dominy, B. N.; Brooks, C. L., III. *J. Phys. Chem. B* **1999**, *103*, 3765–3773.
- (18) Still, W. C.; Tempczyk, A.; Hawley, R. C.; Hendrickson, T. *J. Am. Chem. Soc.* **1990**, *112*, 6127–6129.
- (19) Case, D. A.; Pearlman, D. A.; Caldwell, J. C.; Cheatham, T. E., III; Ross, W. S.; Simmerling, C. L.; Darden, T. A.; Merz, K. M.; Stanton, R. V.; Cheng, A. L.; Vincent, J. J.; Crowley, M.; Tsui, V.; Radmer, R. J.; Duan, Y.; Pitera, J.; Massova, I.; Seibel, G. L.; Singh, U. C.; Weiner, P. K.; Kollman, P. A. *AMBER 6*; University of California: San Francisco, 1999.
- (20) Srinivasan, J.; Trevathan, M. W.; Beroza, P.; Case, D. A. *Theor. Chem. Acc.* **1999**, *101*, 426–434.
- (21) Hawkins, G. D.; Cramer, C. J.; Truhlar, D. G. *Chem. Phys. Lett.* **1995**, *246*, 122–129.
- (22) Sitkoff, D.; Sharp, K. A.; Honig, B. *J. Phys. Chem.* **1994**, *98*, 1978–1988.
- (23) Weiser, J.; Shenkin, P. S.; Still, W. C. *J. Comput. Chem.* **1999**, *20*, 217–230.
- (24) Gohlke, H.; Kiel, C.; Case, D. A. *J. Mol. Biol.* **2003**, *330*, 891–913.
- (25) Zhu, J.; Shi, Y.; Liu, H. *J. Phys. Chem. B* **2002**, *106*, 4844–4853.
- (26) Masunov, A.; Lazaridis, T. *J. Am. Chem. Soc.* **2003**, *125*, 1722–1730.
- (27) Jayaram, B.; Liu, Y.; Beveridge, D. L. *J. Chem. Phys.* **1998**, *109*, 1465–1471.
- (28) Cui, G.; Simmerling, C. *J. Am. Chem. Soc.* **2002**, *124*, 12154–12164.
- (29) Williams, D. J.; Hall, K. B. *Biophys. J.* **1999**, *76*, 3192–3205.
- (30) Pineda De Castro, L. K.; Zacharias, M. *J. Mol. Recognit.* **2002**, *15*, 209–220.

- (31) Harris, S. A.; Gavathiotis, E.; Searle, M. S.; Orozco, M.; Laughton, C. A. *J. Am. Chem. Soc.* **2001**, *123*, 12658–12663.
- (32) Searle, M. S.; Embrey, K. J. *Nucleic Acids Res.* **1990**, *18*, 3753–3762.
- (33) Gavathiotis, E.; Sharman, G. J.; Searle, M. S. *Nucleic Acids Res.* **2000**, *28*, 728–735.
- (34) Berendsen, H. J. C.; Postma, J. P. M.; DiNola, A.; Haak, J. J. *Chem. Phys.* **1984**, *81*, 3684–3690.
- (35) Humphrey, W.; Dalke, A.; Schulten, K. *J. Mol. Graphics* **1996**, *14*, 33–38.
- (36) Sherer, E. C.; Cramer, C. J. *J. Phys. Chem. B* **2002**, *106*, 5075–5085.
- (37) Cornell, W.; Abseher, R.; Nilges, M.; Case, D. A. *J. Mol. Graphics Modell.* **2001**, *19*, 136–145.
- (38) Hess, B. *Phys. Rev. E* **2000**, *62*, 8438–8448.
- (39) Schlitter, J. *Chem. Phys. Lett.* **1993**, *215*, 617–621.
- (40) Egli, M. *Chem. Biol.* **2002**, *9*, 277–286.
- (41) Hud, N. V.; Polak, M. *Curr. Opin. Struct. Biol.* **2001**, *11*, 293–301.
- (42) *Methods in Molecular Biology*; Fox, K., Ed.; Humana Press: Totowa, New Jersey, 1997; p 90.